

CAMBIUM

Circular Material flows in Belgium

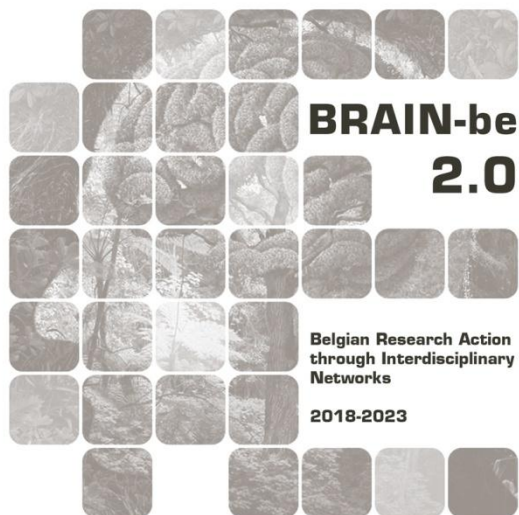
WP4: Case studies on critical material flows

Mapping critical material flows in Belgium: a multilayer material system analysis

Jana Deckers (VITO)
Maarten Christis (VITO)

Pillar 3: Federal societal challenges





NETWORK PROJECT

CAMBIUM

Circular Material flows in Belgium

Contract - B2/223/P3/CAMBIUM

WP 4: Case studies on critical material flows

Mapping critical material flows in Belgium: a multilayer material system analysis

PROMOTORS: Maarten Christis (VITO)
Marco Orsini (ICEDD)

AUTHORS: Jana Deckers (VITO)
Maarten Christis (VITO)





Published in 2023 by the Belgian Science Policy Office
WTCIII
Simon Bolivarlaan 30 bus 7
Boulevard Simon Bolivar 30 bte 7
B-1000 Brussels
Belgium
Tel: +32 (0)2 238 34 11
<http://www.belspo.be>
<http://www.belspo.be/brain-be>

Contact person: Jana Deckers
Tel: +32 (0)14 33 69 29

Neither the Belgian Science Policy Office nor any person acting on behalf of the Belgian Science Policy Office is responsible for the use which might be made of the following information. The authors are responsible for the content.

No part of this publication may be reproduced, stored in a retrieval system, or transmitted in any form or by any means, electronic, mechanical, photocopying, recording, or otherwise, without indicating the reference:

Deckers J., Christis M., **Mapping critical material flows in Belgium: a multilayer material system analysis**. Final Report. Brussels: Belgian Science Policy Office 2025. (BRAIN-be 2.0 - (Belgian Research Action through Interdisciplinary Networks))

TABLE OF CONTENTS

1	INTRODUCTION	5
2	METHODOLOGICAL APPROACH	6
2.1	SYSTEM BOUNDARIES	6
2.2	THE MULTILAYER MATERIAL SYSTEM ANALYSIS	6
2.3	CALCULATIONS, DATA SOURCES AND ASSUMPTIONS.....	8
2.3.1	Installed wind turbines in Belgium and their respective drivetrain technologies	9
2.3.2	The manufacturing phase and trade	9
2.3.3	Use phase	12
2.3.4	Collection phase	13
3	RESULTS AND DISCUSSION	14
3.1	GRANDPARENT AND PARENT LAYER.....	14
3.2	CHILD LAYER.....	17
4	POLICY SUMMARY	24
5	REFERENCES	26
6	ANNEXES	29

1 INTRODUCTION

Complementary to the material-centred perspective adopted in Nelen et al. (2025), this second chapter adopts a technology-based Multilayer Material System Analysis (MMSA) to map critical and strategic material flows in Belgium. While the material-based approach examines the circulation of specific raw materials, a technology-oriented perspective demonstrates how these materials are embodied in components and technological configurations, and how design choices shape future stocks, flows, and end-of-life pathways. The aim of this report is to demonstrate a multilayer MSA methodology applied to the Belgian context, clarify its analytical steps, and provide transferable tools for applying it to other product groups.

Wind turbine technologies were selected as the demonstrator case primarily due to the availability and resolution of data, covering component masses, drivetrain configurations, installation years, and trade flows (HS 850231). The methodology itself, however, is not specific to wind energy; it is intended to be applicable to other CRM-intensive technologies such as photovoltaic modules, batteries and electric vehicles, which are central to Belgium's and Europe's climate-neutrality objectives.

This technology-based perspective gains additional relevance in the context of European wind energy supply chains. Although the EU hosts a strong manufacturing base for major components such as rotor blades, nacelles and towers, led by Germany, Spain, Denmark, France and the Netherlands (RystadEnergy, 2023), the sector remains highly dependent on imported raw materials. While Belgium does not produce complete turbines, its role in specialised component manufacturing and offshore wind infrastructure makes it an important contributor to the overall EU wind energy value chain. Many of these materials are classified as critical, reflecting their economic importance and elevated supply risk, and several, including copper (Cu), nickel (Ni), aluminium (Al) and neodymium (Nd), are additionally deemed strategic for their role in the green and digital transition (Grohol M. and Veeh C., 2023; Carrara et al., 2023). Future wind-energy deployment could significantly intensify material demand, with increases of up to fifteen-fold by 2050, depending on the scenario and the material (European Commission: Joint Research Centre, 2020a).

Despite this growing importance, the interlinkages between technology-specific material cycles and upstream raw-material supply chains remain insufficiently characterised. This knowledge gap complicates the design of effective strategies for securing material supply, improving resource efficiency, and strengthening waste management in Belgium. Achieving a comprehensive understanding requires monitoring both material flows within technologies and their connection to external supply chains. Material Flow Analysis (MFA), rooted in the principle of mass conservation, offers a structured methodology to quantify these flows and inform evidence-based policymaking on sustainable raw-material management (Müller et al., 2014).

To address these gaps, this study applied a multilayer Material System Analysis (MMSA), adapted from the framework originally developed by Matos et al. (2022) for lithium-ion batteries (Matos, C.T. et al., 2020). The method was extended by Godoy León et al. 2025 to wind-energy technologies by differentiating drivetrain configurations and evaluating multiple metals simultaneously. Six key materials, Al, Cu, Fe, Mn, Ni and Nd, were examined, selected both for their critical and strategic status and for the availability of reliable data. The strength of the multilayer approach lies in its ability to capture potential interconnections between different material cycles, identify bottlenecks across layers, and highlight opportunities to improve supply security and circularity in the Belgian wind-energy sector.

2 METHODOLOGICAL APPROACH

2.1 SYSTEM BOUNDARIES

This study performs a multilayer Material System Analysis (MMSA) for wind turbines in Belgium based on the methodology described by León et al. 2025, focusing on the evolution of material stocks and flows between 1996 and 2021 (Godoy León et al., 2025). While the assessment was conducted for the period between 1996 and 2021, the year 2015 is discussed in more detail due to the wide availability of detailed data on wind turbine specifications, including material intensities, drivetrain configurations, and nominal power ratings. Extending the analysis to 2021 allows for an assessment of how these material flows developed in a more recent context, aligned with Belgium's national wind-energy deployment trends and broader European developments.

The geographical system boundary is restricted to Belgium, considering all wind turbines installed within the Belgian territory as well as the associated import and export flows relevant to the Belgian market. Both onshore and offshore wind turbines are included, encompassing the main components of the turbine system: rotor, nacelle, tower, and foundation. As in similar studies, inter-array and export cables, offshore substations, and grid infrastructure are excluded from the analysis, as they fall outside the scope of the turbine-specific material system. From a technological perspective, the assessment distinguishes between two major wind turbine drivetrain types, Gearbox (GB) and Direct-Drive (DD), owing to their different component structures and material compositions. This differentiation is crucial for accurately capturing variations in the use of metals across drivetrain technologies. The material scope covers six metals of relevance for Belgium's critical-raw-material context: aluminium (Al), copper (Cu), iron (Fe), manganese (Mn), nickel (Ni), and neodymium (Nd). These materials were selected because of their strategic importance for low-carbon technologies and, in the case of Fe, because of its dominant presence in wind turbine structures and its role as an essential steel constituent, despite not being classified as a CRM. The materials embedded in electrics and electronics were not included in this analysis.

The analysis adopts a life-cycle perspective spanning manufacturing, installation, operation (including repairs and replacements), and end-of-life treatment. It covers both recycling pathways and waste disposal generated across these stages. These system boundaries ensures that all major flows and stocks of the selected materials within Belgium's wind-energy system are consistently accounted for.

2.2 THE MULTILAYER MATERIAL SYSTEM ANALYSIS

The methodological approach of this study is based on a Material System Analysis (MSA), a methodology situated within the broader framework of Material Flow Analysis (MFA) and used by the European Commission to support raw-material policy development. The MSA approach was first established for the EU in 2015 (BIO by Deloitte, 2015) and later refined (European Commission: Joint Research Centre, 2020b). It defines consistent system boundaries across life-cycle stages, including production, trade, use, and end-of-life, and quantifies all major flows and stocks of raw materials based on the principle of mass conservation. The framework also captures relevant stocks in products, landfills, and tailings.

In this study, and in accordance with the methodology described by Godoy León et al. (2025), the MSA framework is extended to wind turbine technologies using a multilayer system approach, applied to the six selected metals with wind power technologies serving as the central integrating element. The multilayer structure consists of:

- **Grandparent layer** – flows and stocks of the complete technology (wind turbines), including: material composition, trade, and market developments.

- **Parent layer** – flows and stocks of distinct applications or technology types. In this case, the differentiation is made between gearbox (GB) and direct-drive (DD) wind turbines.
- **Child layer** – flows and stocks of each selected material.
- **Lower layers** – (i) flows and stocks of the selected materials within the complete technology, and (ii) flows and stocks of the same materials across the wider market. These lower layers allow comparison between technology-specific material dynamics and broader supply-chain behaviour.

A schematic overview of the applied layer structure is depicted in **Figure 1** for the Belgian wind turbine system (grandparent layer), with separate consideration of GB and DD turbines (parent layer). In both the grandparent and parent layers, all materials incorporated into wind turbines are quantified except concrete. Concrete represents a substantial share of total mass, often more than 80 % for onshore turbines, and is excluded here to concentrate the analysis on the selected metals. Likewise, materials used in offshore scour protection are omitted, as they fall outside the core turbine system. Within the parent layer, GB and DD technologies are examined separately due to their distinct component configurations and material intensities. Gearbox turbines encompass a range of generator–drivetrain combinations, including:

- high-speed Squirrel Cage Induction Generator (SCIG) (type A, F),
- high-speed Wound Rotor Induction Generator (WRIG) (type B),
- high-speed Doubly-Fed Induction Generator (DFIG) (type C),
- medium/high-speed Electrically Excited Synchronous Generator (EESG) (type E-EE),
- medium/high-speed Permanent Magnet Synchronous Generator (PMSG) (type E-PM).

Direct-drive turbines include low-speed systems such as:

- EESG (type D-EE), and
- PMSG (type D-PM).

This level of technological differentiation enables a more accurate representation of material composition and flow dynamics across Belgium’s wind turbine fleet.

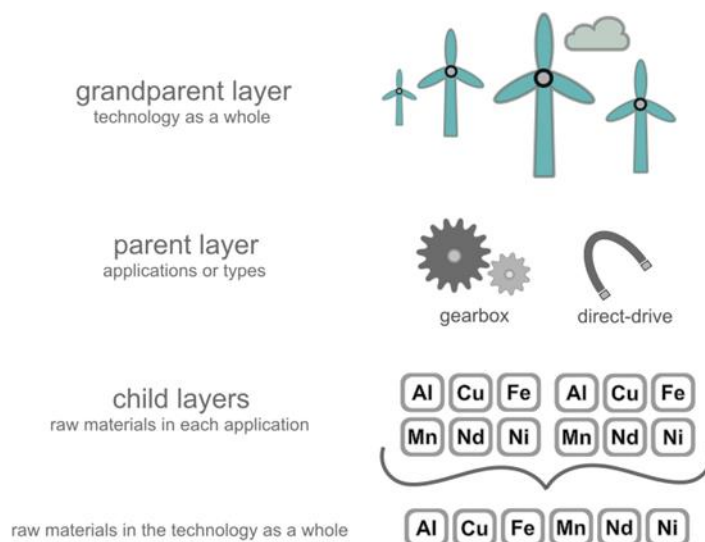


Figure 1 Schematic overview of the applied layer structure

2.3 CALCULATIONS, DATA SOURCES AND ASSUMPTIONS

This section describes the flows that were considered for the MMSA. The calculations are detailed together with the consolidated data sources and underlying assumptions. The notation of the flows adheres to the original MSA framework and are structured according to the life-cycle stages to which they pertain (manufacturing to recycling). The layers of the multilayer structure are also specified. For clarity and transferability, the description of the flows is presented following the logical workflow used to populate the MMSA, enabling straightforward adaptation to other technologies. The considered material flows are summarized in **Table 1** and **Figure 2**.

Table 1: Overview of the considered material flows.

Flows	
To manufacturing	M2.1
Man. Waste	D1.4
To reprocessing	D1.5
To market 3	D1.1
Import market 3	E1.4
Export market 3	D1.2
To use	M3.1
To collection	E1.6
Waste from collection	F1.3
To recycling	F1.4
Recycled	G1.1 + G1.2
Export	G1.3
Non-functionally recycled	G1.4
Waste from recycling	G1.5
Stocks	
Addition to in-use	E1.7
Stock of in-use	E1.1
Addition to landfill	F1.6
Landfill stock	F1.5
Accumulated downcycled material	G1.6

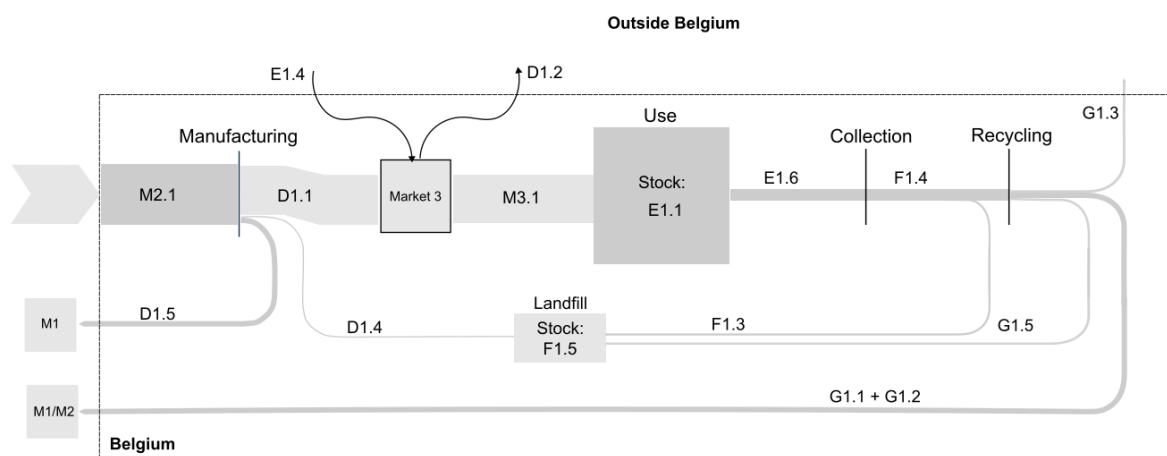


Figure 2: Schematic overview of the considered material flows.

2.3.1 Installed wind turbines in Belgium and their respective drivetrain technologies

Before constructing the MMSA, a comprehensive and robust dataset was compiled, covering the number of wind turbines installed in Belgium, their model and manufacturer, nominal power rating, location (onshore or offshore), year of installation and decommissioning, and drivetrain type. These data were systematically cross-validated using publicly available information on Belgian wind farms. For this purpose, an extensive dataset from Windpower was obtained and used as the primary reference. The turbine models listed in this dataset were manually matched to their corresponding drivetrain technologies through cross-checks with publicly accessible technical databases, including *wind-turbine-models.com* and *thewindpower.net*. This ensured accurate drivetrain classification and improved the reliability of the subsequent multilayer MSA.

2.3.2 The manufacturing phase and trade

The following mass balance was used to estimate the total mass going to manufacturing:

$$M2.1 = D1.1 + D1.4 + D1.5$$

In this mass balance D1.1 represents the flow of manufactured products leaving the manufacturing phase:

$$D1.1 = M3.1 + D1.2 - E1.4$$

Where D3.1 is the flow products entering the use phase in Belgium and D1.2 and E1.4 represent, the exported and imported products respectively.

Firstly, the flow M3.1 was determined as:

$$M3.1 = \sum_{j=1}^2 \sum_{n=1}^7 NC_j \cdot \eta_{j,n} \varphi_n + \sum_{j=1}^2 \sum_{n=1}^7 F_{j,n}$$

Where:

- NC_j = newly installed capacity for j;
- j = 1: onshore, j = 2: offshore;
- n = type of installed technologies (GB-SCIG, GB-DFIG, GB-EESG, GB-PMSG, DD-PMSG and DD-EESG) for onshore and offshore;
- $\eta_{j,n}$ = is the percentage of newly installed technologies;
- φ_n = material intensity per drivetrain technology;
- $F_{j,n}$ = the material requirements for repair and replacement per drivetrain technology.

The considered material intensities per drivetrain technology were adopted from (Carrara et al., 2023; Farina and Ancitil, 2022) and are depicted in **Table 2**.

Table 2: Material intensities (t/GW) per drivetrain technology. The material intensity of the GB-DFIG drivetrain is set equal to the material intensity of the GB-DFIG technology (Carrara et al. 2020).

	GB-DFIG	GB-PMSG	DD-EESG	DD-PMSG
Al	1,400	1,600	700	500
Cu	1,400	950	5,000	3,000
Fe	0	30	300	300
Nd	12	51	28	180
Steel – low alloy	15,522-474,333	14,697-44,914	18,131-55,408	16,414-50,161

Steel – high alloy	11,295-5,006	10,695-4,740	13,194-5,848	11,944-5,294
Steel-unalloyed	66,463-0	62,934-0	23,037-70,744	20,856-64,045
Cast iron	18,000	20,800	20,100	20,100

For the different types of steel and cast iron which constitute a large proportion of the wind turbines, different metal compositions were used and are shown in **Table 3**. Steel containing chromium is hereafter referred to as high-alloyed steel.

Table 3: Metal composition of different types of steel (%w/w).

	Fe	Al	Cu	Ni	Mn	Nd	Reference
Steel – low alloy	96.0%	0.02%	0.55%	0.33%	1.60%	0.00%	Arcelormittal (2024)
Steel – chromium	68.5%	0.10%	0.00%	10.00%	2.00%	0.00%	EngineerExcel (2023)
Steel – unalloyed	97.6%	0.00%	0.00%	0.40%	0.65%	0.00%	Thyssenkrupp (2023)
Cast iron	94.1%	0.00%	0.00%	0.00%	0.65%	0.00%	ELSAwy et al. (2017), Reliance foundry (2020)

The newly installed capacity by drivetrain type, for both onshore and offshore wind turbines, was derived from the compiled Belgian installation dataset in combination with drivetrain-specific shares identified for each commissioning year. As described earlier, the MMSA framework extends beyond the quantification of material requirements for primary manufacturing and accounts for material inputs associated with component repair and replacement during the use phase. The analysis assumes that, apart from turbines imported as complete units, wind turbines installed in Belgium are (re)manufactured domestically. Although this assumption does not fully reflect actual manufacturing practices, the resulting indicator provides a meaningful estimate of the material flows entering the Belgian economy in the form of wind turbines and their constituent components.

To estimate these additional material requirements, the mass of each turbine component was first determined. This was achieved using the upscaling method proposed by Shammugam et al. (2019), which links component mass to rotor diameter through empirically derived scaling relationships (Shammugam et al., 2019). The method is based on the following equation:

$$\log_{10}(M) = \log_{10}(a) + b \cdot \log_{10}(D)$$

Where:

- D = rotor diameter (m);
- M = component mass (ton);
- log(a) and b = upscaling parameters derived from historical turbine datasets and engineering models.

Shammugam et al. 2019 compiled mass–diameter correlations for major turbine components (e.g., pitch system, yaw system, gearbox, generator types, nacelle structures, rotor, tower) by fitting these parameters to a large population of commercially available turbines between 1980 and 2015. In this study, the rotor diameter for each year (**Annex A: Table 8**) is used as a proxy for the scaling of component masses, under the assumption that rotor size is a reliable indicator of turbine size and consequently of component mass. The corresponding upscaling parameters are summarised **Table 4** and **Table 5**.

Table 4: Upscaling factors for mass according to Schammugam et al. 2019.

	log(a)	b
Rotor	-3.34	2.56
Nacelle		
DFIG	-2.28	2.13
PMSG-DD	-3.40	2.7
PMSG-GB	-2.27	2.15
EESG-DD	-3.29	2.7
SCIG	-1.24	1.59
Tower	-4.22	3.22

Table 5: Replacement and repair rates per component together with the required material need per type of repair or replacement according to Schammugam et al. 2019.

	major replacement rate	major repair rate	minor repair rate
pitch	0.001	0.179	0.824
yaw	0.001	0.006	0.162
gearbox	0.051	0.036	0.369
generator DFIG - GB	0.109	0.356	0.538
generator PMSG - DD	0.009	0.030	0.546
generator PMSG - GB	0.008	0.025	0.455
generator EESG - DD	0.109	0.356	0.538
generator SCIG - GB	0.109	0.356	0.538
Material requirement	1.000	0.200	0.100

Table 6: Upscaling factors for failure according to Shammugam et al. 2019.

	log(a)	b
Pitch	-4.26	2.54
Yaw	-5.83	3.31
Gearbox	-2.52	1.99
Generator		
DFIG	-2.15	1.61
PMSG-DD	-1.30	1.61
PMSG-GB	-2.06	1.61
EESG-DD	-1.15	1.61
SCIG	-2.15	1.61

Once the mass per component was estimated for each drivetrain technology and installation year, failure parameters (**Table 6**) were applied. These parameters represent the annual probability of major replacement, major repair, or minor repair for specific components together with the material requirements per type of repair or replacement. Failure rates are only provided for the pitch system, yaw system, gearbox, and generator. Components such as the tower, nacelle housing, and rotor blades were excluded from the failure analysis because their failure typically leads to end-of-life decommissioning rather than repair or replacement. For each drivetrain type, the material required for maintenance was calculated by summing up the relevant component flows across all failure categories.

$$F_{j,l} = \sigma_{k,l} \cdot \theta_k \cdot \sum_{t=1}^{\text{assessed year}} T_{j,t} \cdot m_{l,t}$$

Where:

- $\sigma_{k,l}$ = the rate of replacement for k: major replacement, major repair, or minor repair, per component l;

- θ_k = the percentage of material that needs to be replaced or repaired;
- $T_{j,t}$ is the number of new turbines installed in year t ;
- $m_{l,t}$ is the upscaled mass of component l for year t .

Material intensities (wt%) for the total wind turbine and for each drivetrain configuration were derived using the component-level material composition data (Annex A **Table 8**) for the assemblies considered: rotor, nacelle, and tower. To translate these material percentages into mass-based intensities, the annual installed mass per component, calculated using the Shammugam upscaling method, was multiplied by the corresponding material weight fractions and normalised to the total component mass. Summing these contributions across components yielded material intensities at the parent level (GB vs. DD) and at the grandparent level (the total wind turbine).

Secondly, the export (D1.2) and import (E1.4) flows were determined. Therefore, export and import flows were obtained from Eurostat COMEXT using HS 850231 (wind-powered generating sets). Import and export volumes (kg) were allocated across drivetrain technologies based on the drivetrain distribution observed in the European fleet outside Belgium (for export) and based on the drivetrain distribution of installed capacity within Belgium (for imports).

Material intensities (wt%) for the total wind turbine and for each drivetrain configuration were derived using the component-level material composition data (Annex A **Table 8**) for the assemblies considered: rotor, nacelle, and tower. To translate these material percentages into mass-based intensities, the annual installed mass per component—calculated using the Shammugam upscaling method—was multiplied by the corresponding material weight fractions and normalised to the total component mass. Summing these contributions across components yielded material intensities at the parent level (GB vs. DD) and at the grandparent level (the total wind turbine).

These material compositions were subsequently applied to the import and export volumes to quantify flows D1.2 and E1.4 at the child layer, i.e., for each individual metal under consideration.

Finally, flows D1.4 (manufacturing waste) and D1.5 (secondary material to reprocessing) were estimated as follows:

$$D1.4_i = \frac{D1.1}{1-\omega_i-\sigma_i} \cdot \omega_i \rightarrow D1.4 = \sum_i D1.4_i$$

$$D1.5_i = \frac{D1.1}{1-\omega_i-\sigma_i} \cdot \sigma_i \rightarrow D1.5 = \sum_i D1.5_i$$

Where:

- ω_i = the percentage of manufacturing losses;
- σ_i = the percentage of scrap that comes back to the processing phase for reprocessing.

2.3.3 Use phase

The in-use stock (E1.1) was determined based on the yearly newly installed capacity:

$$E1.1 = \sum_{j=1}^2 \sum_{t=1997}^{2015 \text{ or } 2021} \sum_{n=1}^7 NC_{j,t,n} \cdot \varphi_n$$

Where:

- $NC_{j,t,n}$ = newly installed capacity (MW) for both onshore and offshore per year, per drivetrain technology;
- φ_n = material intensity per drivetrain technology (t/MW).

The newly installed capacity for both onshore and offshore per year, per drivetrain technology could be derived from the compiled dataset. Hence the parent and grandparent layer could be derived from these empirical data.

2.3.4 Collection phase

The flow of products collected at EoL (E1.6) was calculated by estimating contributions from decommissioned wind turbines (E1.6_A) and failure of components (E1.6_B):

$$E1.6_B = \sum_j \sum_l F_{j,l}$$

For all three layers, it was assumed that end-of-life (EoL) wind turbines are neither imported nor exported. When a decommissioning year was reported in the dataset, this value was used directly. For turbines without a disclosed decommissioning date, an average operational lifetime of 18 years was assumed.

To compute E1.6_B at the parent layer (drivetrain), the total mass of failures was estimated for the components that are specific to each drivetrain type. For components shared by both drivetrain configurations—such as the pitch and yaw systems—failures were allocated proportionally by multiplying the total number of newly installed turbines by the yearly share of newly installed GB versus DD turbines. To allocate the mass of failures and decommissioned turbines to the materials of interest, the mass percentages per component, as defined by Shammugam et al. (2019) were used (Annex A **Table 8**).

In the recycling stage, the material quantities directed towards recycling (F1.4) were determined for each of the six metals of interest. Consistent with the European MSA methodology, the analysis distinguishes between functional recycling, where materials retain similar quality and utility, and downcycling, where material quality is reduced. Functional recycling is hereafter referred to as recycling. To estimate the mass that is recycled, recycling efficiencies from Demuytere et al. (2024) (**Table 7**) were applied. These efficiency values were assumed to remain constant across the analysed years (Demuytere et al., 2024).

Table 7: Material recycling efficiencies (%). Steel adopted from Pauliuk et al., 2017; Fe and cast iron adopted from Cullen et al. (2012); Cu adopted from Andersen et al. (2014); Al adopted from International Aluminium Institute (2020); Polymers adopted from Kawecki et al., 2018. For the different types of steel the same efficiency was assumed. Since Nd and “others” are not recycled, they are not shown.

Material	Recycling efficiency (%)
Steel	90.4
Fe and cast iron	98.5
Cu	98.0
Al	76.0
Polymers	59.0

The amount of recycled material that is exported (G1.3) was calculated by applying an export rate of 17%, based on Rostek et al. (2022), which represents the average fraction of steel scrap exported from the EU. This export share was assumed to remain constant throughout the analysed period.

The accumulation of material in landfill stock (F1.5) was determined by summing all material flows directed to landfill over the entire assessment period. This reflects the cumulative nature of landfill stocks, which continue to increase unless material is removed, which is not the case for wind turbine materials.

$$F1.5_T = \sum_{t=t_0}^T F1.6_T$$

At the child layer, the metal composition values provided in **Table 3** were applied to distribute these flows across the six individual metals considered in this study.

3 RESULTS AND DISCUSSION

3.1 GRANDPARENT AND PARENT LAYER

Throughout this section the results of the MMSA are discussed with a specific focus on 2015 and 2021, the results for other assessed years are available upon request. The analysis is structured per MMSA layer, beginning with the grandparent and parent layers, followed by the child layer, which examines the selected materials and their linkages to the relevant drivetrain technologies.

Figure 3 and **Figure 4** presents the results for the grandparent and parent layers for 2015 and 2021. In 2015, approximately 61,036 tonnes of materials entered the manufacturing phase. During manufacturing, 8,606 tonnes were directed to reprocessing (Market 1), while 1,511 tonnes were considered manufacturing waste, assumed to be destined for landfill. This corresponded to an overall manufacturing yield of 83%, with 50,918 tonnes of embedded materials entering Market 3. In addition, 346 tonnes of materials were estimated to be imported embedded in wind turbines (HS 85231) while 484 tonnes were exported which amount to a net export of 138 tonnes. Imported wind turbines were assumed to be installed domestically. Since the trade of components is not considered in this analysis this most likely an underestimation of the imported and exported materials.

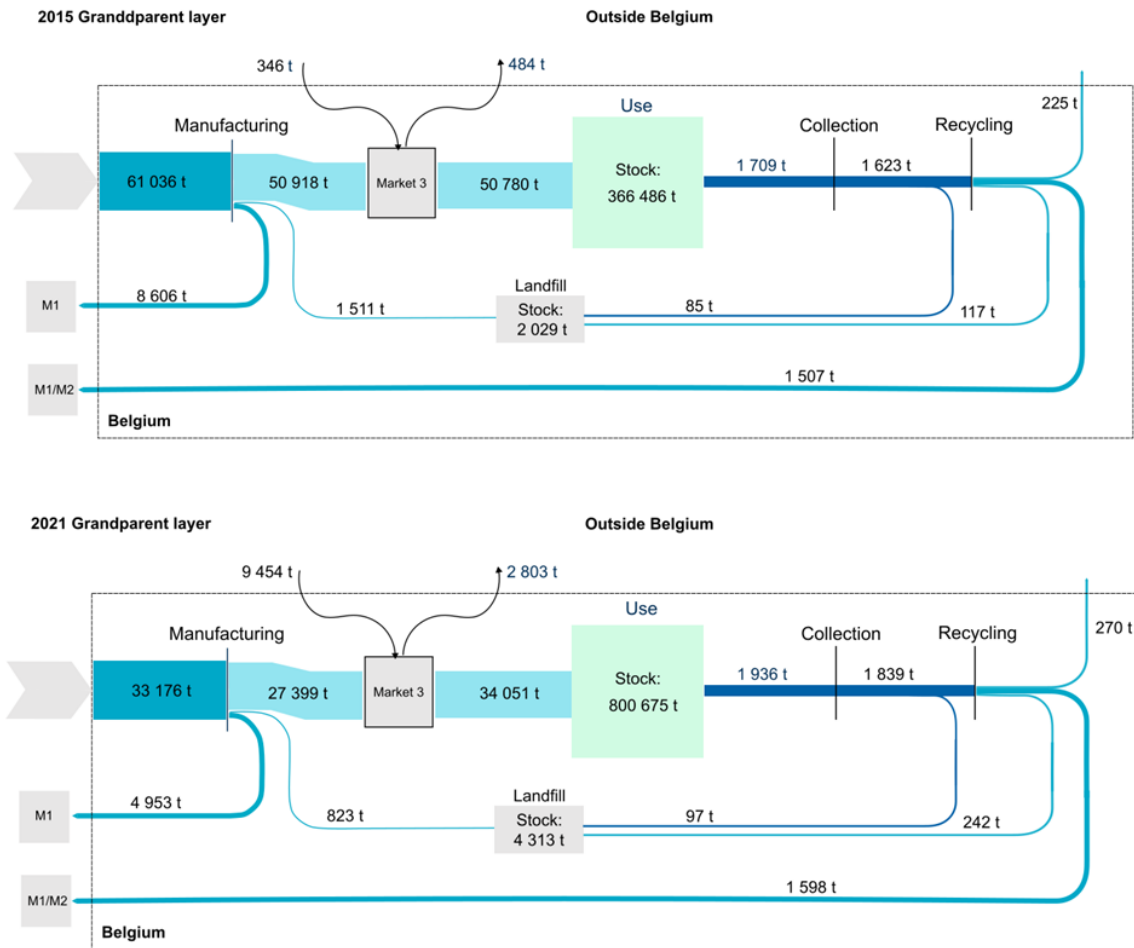


Figure 3: Grandparent layer for stock and flows of materials linked to wind turbines in Belgium in 2015 and 2021. M1: Market 1, M2: Market 2. These corresponds to the markets before and after processing. The arrows represent flows inside Belgium, coming from Market 2. Downcycling flows are not shown due to their low values. Flows and stocks are shown in tonnes (t).

Based on drivetrain shares, 54% of materials embedded in wind turbines put on the Belgian market were associated with GB technologies, while 46% were associated with DD technologies. In total, 27,221 tonnes of materials entered the use phase embedded in GB turbines and 23,560 tonnes in DD turbines. These additions contributed to an in-use stock of 366 477 tonnes, of which 227,707 tonnes originated from GB and 138,770 tonnes from DD installations.

It was estimated that 1,709 tonnes of materials left the use phase through decommissioning, failures and repairs. According to the consolidated dataset, one wind turbine was decommissioned in 2015, corresponding to 38.6 tonnes of materials (GB technology). Of the materials leaving the use phase, 95 % was assumed to be directed to high-end recycling, hence 86 tonnes was estimated to be waste from collection. Approximately 93 % of the material was recovered, with 1,506 tonnes returning to Market 1 (pre-processing) or Market 2 (premanufacturing), and 255 tonnes was estimated to be exported. The remaining 117 tonnes was assumed to be disposed of in landfill. Of the recycled output, 34 % originated from GB wind turbines and 66 % from DD turbines. The accumulated landfill stock was estimated to be 535 tonnes, comprising 166 tonnes from GB wind turbines and 369 tonnes from DD wind turbines.

Between 2015 and 2020, material flows and stocks associated with wind turbines increased substantially. In 2020, approximately 136,988 tonnes of materials were directed to the use phase, linked to the installation of 132 turbines, including 81 offshore DD-PMSG machines. In 2021, the number of newly

installed turbines dropped to around 60. The drivetrain shares fluctuated considerably during the assessed period; however, in-use stocks of DD technologies more than doubled, while GB in-use stock roughly doubled as well.

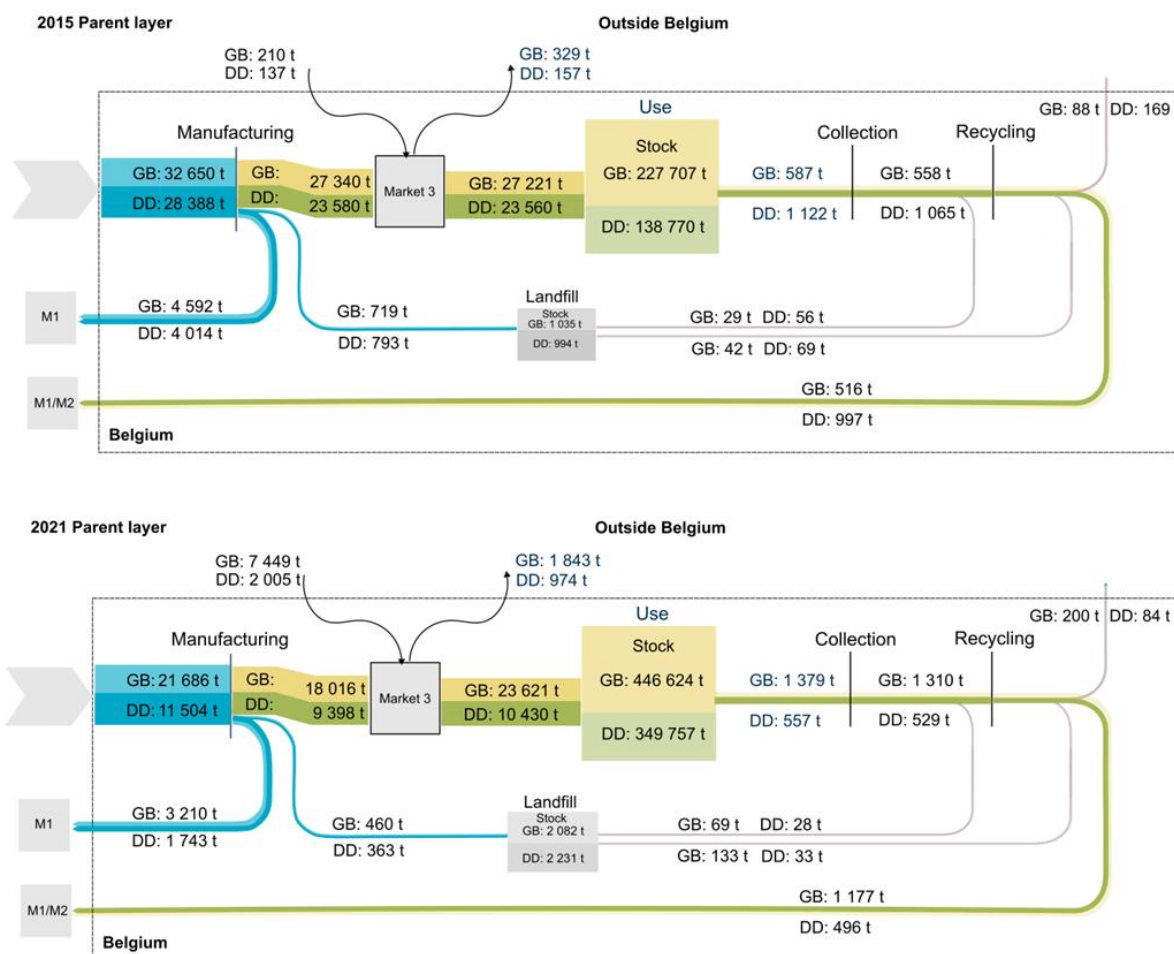


Figure 4: Parent layer for stock and flows of materials linked to wind turbines and, more specifically, the corresponding drivetrain technologies in Belgium in 2015 and 2021. M1: Market 1, M2: Market 2. These corresponds to the markets before and after processing. The arrows represent flows inside Belgium, coming from Market 2. Downcycling flows are not shown due to their low values. Flows and stocks are shown in tonnes (t). GB: Gearbox, DD: Direct-drive.

As highlighted by Godoy León et al. (2025), DD technology has gained prominence due to the vulnerability of gearboxes to stress induced by wind turbulence, which can lead to component degradation and mechanical failure. This susceptibility becomes more pronounced at higher wind speeds, making gearboxes particularly critical in offshore environments. Conversely, onshore wind farms continue to rely more heavily on GB turbines because DD systems are generally larger and more expensive, limiting their competitiveness in cost-sensitive and space-constrained onshore settings (Godoy León et al. 2025).

From a technological standpoint, in 2015, 57% of newly installed turbines were GB, while 43% were DD. On average, 60% of onshore and 57% of offshore installations applied GB technology in 2015, resulting in a somewhat higher mass embedded in GB turbines. As noted earlier, however, this distribution varies strongly across years, particularly for offshore installations, which are typically installed in larger project batches rather than through continuous deployment.

3.2 CHILD LAYER

This section presents and discusses the child-layer results, providing a detailed comparison of the material cycles and system behaviour of the six individual metals used in wind turbine technologies. The flows and stocks for the different materials are shown for 2015 and 2021 in **Figure 5**, **Figure 6**, **Figure 7**, and **Figure 8**. Because of the differences in magnitudes the figures are subdivided showing the flows for the shows for both Fe and Cu separately from Ni, Mn, and Al. The results for Nd are shown in **Figure 8**.

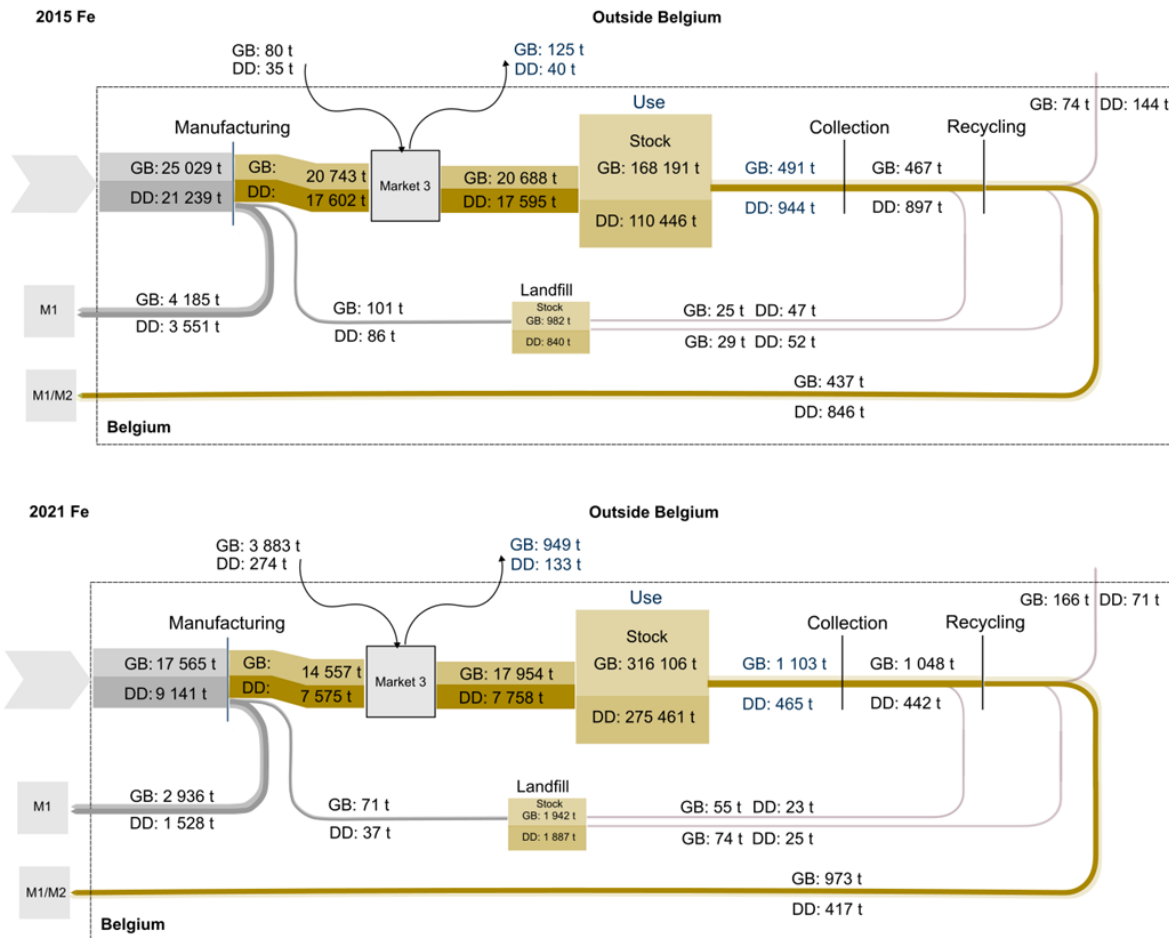


Figure 5: Child layer for stock and flows of iron (Fe) linked to wind turbines and, more specifically, the corresponding drivetrain technologies in Belgium in 2015 and 2021. M1: Market 1, M2: Market 2. These corresponds to the markets before and after processing. The arrows represent flows inside Belgium, coming from Market 2. Downcycling flows are not shown due to their low values. Flows and stocks are shown in tonnes (t). GB: Gearbox, DD: Direct-drive.

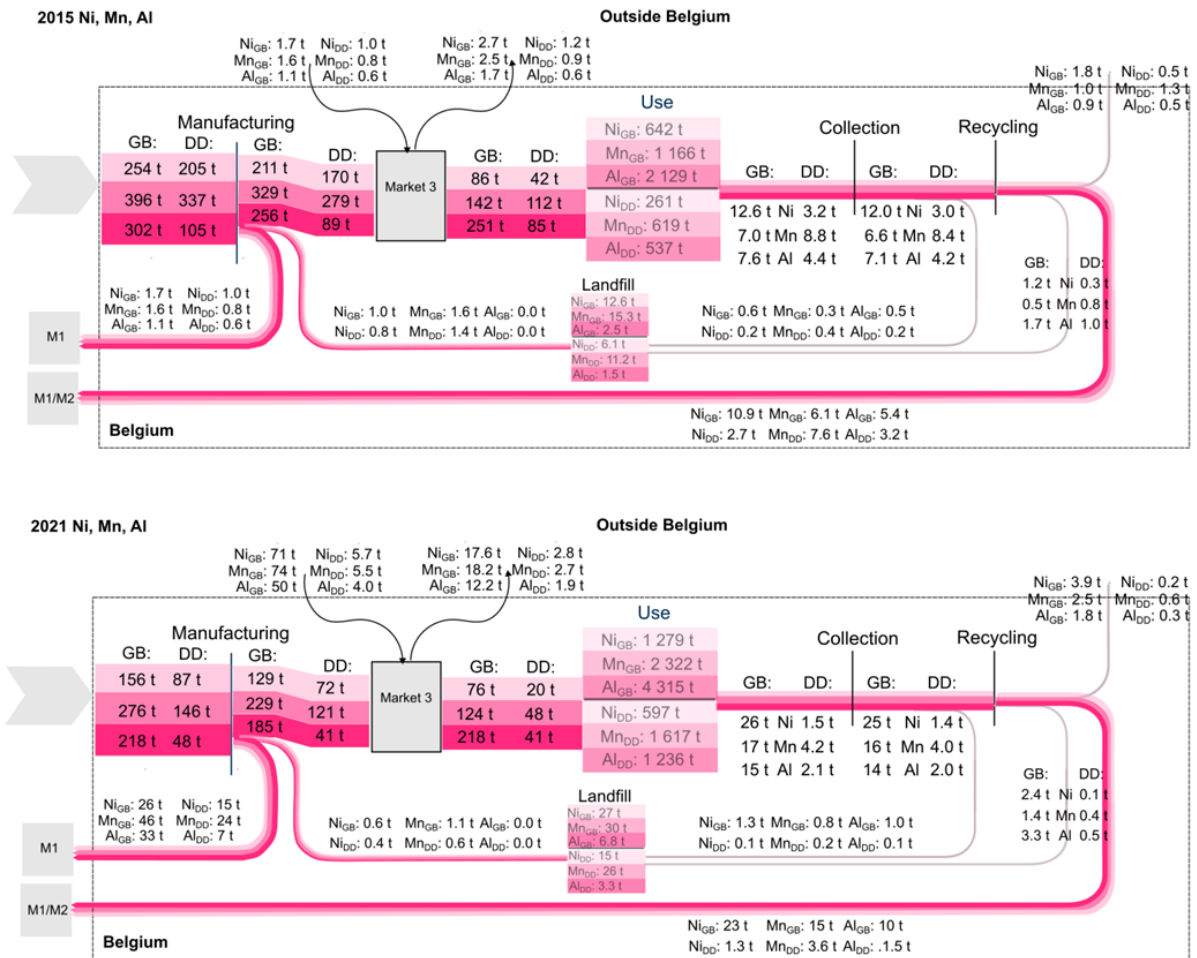


Figure 6: Child layer for stock and flows of nickel (Ni), manganese (Mn) and aluminium (Al) linked to wind turbines and, more specifically, the corresponding drivetrain technologies in Belgium in 2015 and 2021. M1: Market 1, M2: Market 2. These corresponds to the markets before and after processing. The arrows represent flows inside Belgium, coming from Market 2. Downcycling flows are not shown due to their low values. Flows and stocks are shown in tonnes (t). GB: Gearbox, DD: Direct-drive.

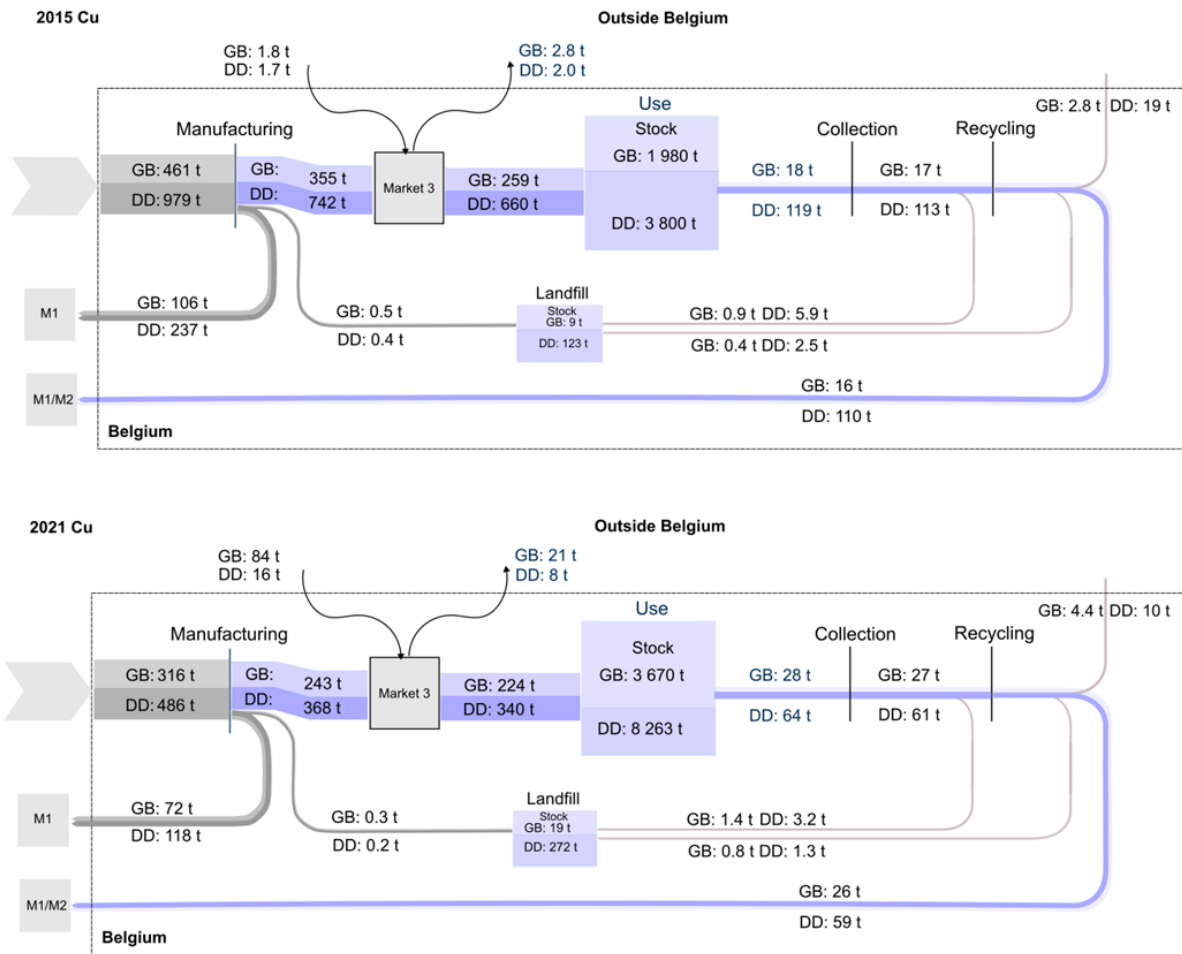


Figure 7: Child layer for stock and flows of copper (Cu) linked to wind turbines and, more specifically, the corresponding drivetrain technologies in Belgium in 2015 and 2021. M1: Market 1, M2: Market 2. These corresponds to the markets before and after processing. The arrows represent flows inside Belgium, coming from Market 2. Downcycling flows are not shown due to their low values. Flows and stocks are shown in tonnes (t). GB: Gearbox, DD: Direct-drive.

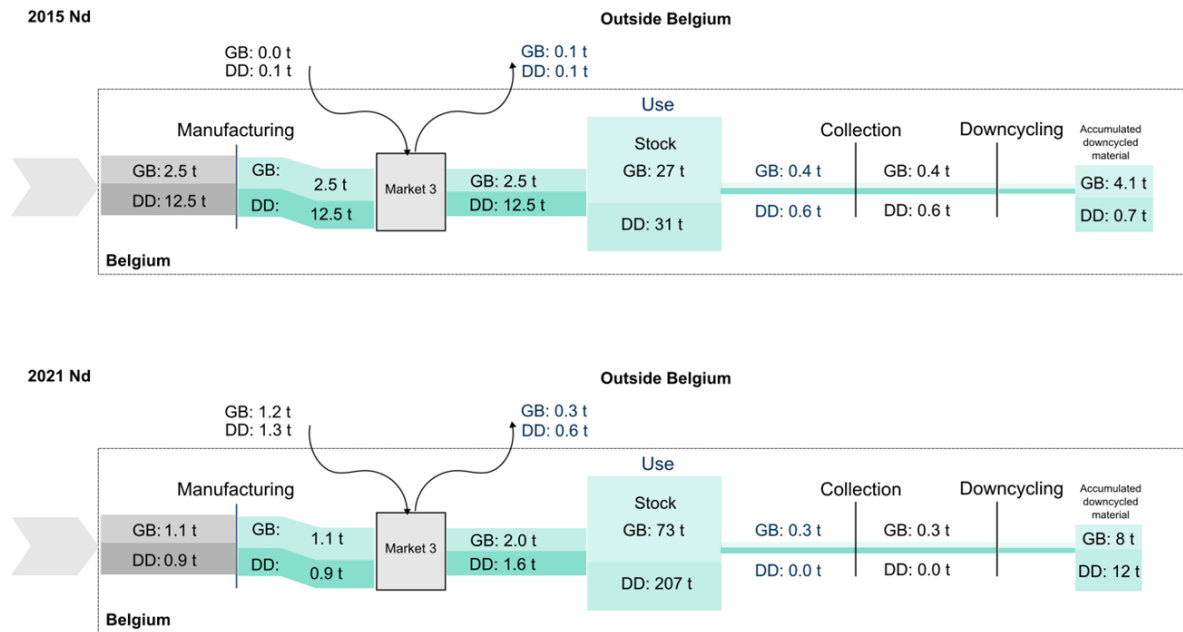


Figure 8: Child layer for stock and flows of *neodymium (Nd)* linked to wind turbines and, more specifically, the corresponding drivetrain technologies in Belgium in 2015 and 2021. M1: Market 1, M2: Market 2. These corresponds to the markets before and after processing. The arrows represent flows inside Belgium, coming from Market 2. Downcycling flows are not shown due to their low values. Flows and stocks are shown in tonnes (t). GB: Gearbox, DD: Direct-drive.

The relation of Fe embedded in GB and DD turbines is similar to the relation of the total mass. For instance, of the total Fe going to the manufacturing phase, 54% is associated with GB turbines and 46% with DD turbines. This ratio remains relatively constant up to the use phase. A similar trend is observed for Ni and Mn, although León indicates that these differences became more pronounced for these metals due to variations in steel types. The fact that this does not clearly emerge in our analysis may reflect differences in the material intensity assumptions used for steel. However, since high-alloyed steel, containing the highest Ni percentage, is used slightly more in DD turbines, the reasoning of Godoy León et al. (2025) is not entirely evident, and a less pronounced difference is expected when following this reasoning. In our study, an average of the steel-related material intensities for offshore and onshore turbines was applied, which may have smoothed out the underlying differences between drivetrain types.

Nevertheless, a more pronounced difference is observed for Al: up to the use phase, approximately 74% in 2015 of Al flows are related to GB turbines, reflecting the higher aluminium intensity of GB technologies. Copper shows the opposite behaviour: Cu flows associated with DD technology are 2 to 2.5 times higher than those for GB, consistent with the substantially higher copper intensity in DD systems. This higher copper demand is primarily driven by the generator design: DD turbines rely on low-speed generators with large diameters and high pole counts, which require extensive copper windings to produce sufficient magnetic flux without the use of a gearbox. In contrast, GB turbines employ high-speed induction or double-fed generators, where the gearbox increases rotational speed, allowing for more compact generators with lower copper content. As a result, the absence of a gearbox in DD technologies shifts part of the electromagnetic requirements directly to the generator, thereby increasing the copper intensity (Carrara et al. 2020; Godoy León et al. 2025). Furthermore, the lower shares of aluminium in DD, can be explained by the fact that Cu is still the preferred material for DD turbines. Although there are continued efforts to replace copper with aluminium to reduce both weight

and cost, aluminium still faces several limitations, including lower electrical conductivity, reduced mechanical strength, greater susceptibility to relaxation, and less favourable corrosion resistance (BBF Associates and Kundig, 2011).

Similar patterns are observed for 2021: approximately 65% of the Fe, Ni, and Mn entering the manufacturing phase is associated with GB turbines, consistent with the share of newly installed GB capacity. The difference is again more pronounced for aluminium, with 84% of Al entering the use phase linked to GB installations. In contrast, despite twice as many GB turbines being installed in 2021, the share of Cu embedded in DD turbines remains higher, reflecting their significantly greater copper intensity.

For neodymium (Nd), the material flows show a marked predominance of direct-drive (DD) turbines. Across the life cycle up to the use phase, approximately 85–90 % of Nd ends up in DD configurations, whereas only a minor share is associated with gearbox (GB) turbines. This is consistent with the considerably higher Nd intensity of direct-drive permanent-magnet (DD-PM) systems.

Beyond the use phase, the relative contribution of DD decreases slightly: about 60 % of Nd in end-of-life (EoL) flows originates from DD turbines, while the remainder comes from GB installations. Conversely, the in-use stock contains a larger fraction of Nd in GB turbines, around 45 % in 2015 which decreased to 26 % in 2021. This reflects the long historical dominance of GB turbines in the Belgian and European markets, GB installations have been deployed in larger numbers and have been operating for a longer period, which increases their accumulated stock relative to DD technologies that only expanded more recently.

To assess temporal changes, 2020 was used as the reference comparison year rather than 2021. The data for 2021 showed atypical fluctuations likely related to post-COVID-19 effects, including project delays, partial commissioning, and supply-chain interruptions. Because of this irregularity, 2020 provides a more representative basis for identifying structural trends. Between 2015 and 2020, Nd flows to the use phase increased substantially for both drivetrain types. For GB turbines, Nd entering the use phase rose from around 2.5 tonnes to nearly 13 tonnes, while DD installations exhibited even more pronounced growth, increasing from approximately 12.5 tonnes to over 95 tonnes. Throughout the same period, the in-use stock nearly tripled for GB and increased by six-fold for DD. Concurrently, end-of-life flows of Nd increased sharply. For GB turbines, EoL flows more than doubled between 2015 and 2020, while for DD turbines Nd flows started to emerge, rising from negligible levels in 2015 to more than 6 tonnes by 2020.

Despite these growing flows, Nd remains unrecovered in current waste management systems. NdFeB magnets are typically fragmented during shredding, and the magnetic fraction tends to attach to ferrous scrap streams. These mixed ferrous fractions are subsequently processed in steel recycling, where Nd is diluted into secondary steel or ends up in smelter slag, with no functional recovery (Darcy et al., 2013; Yang et al., 2017). Although wind turbines offer relatively easy access to large permanent magnets compared with other Nd-containing products, persistent low Nd prices and the historically limited availability of end-of-life magnets have hindered the emergence of dedicated recycling routes. As a result, Nd flows in wind turbine end-of-life processing continue to be dissipative rather than circular (Godoy León et al. 2025).

The analysis of Belgian E1.6 flows, representing materials reaching end-of-life through failure, replacement, or decommissioning, reveals a clear and sustained upward trend across all six metals considered in the MMSA (Fe, Cu, Al, Mn, Ni, and Nd). Although the annual flows exhibit pronounced year-to-year variability, reflecting the project-based and irregular nature of wind turbine deployment in Belgium, particularly for offshore installation, the underlying long-term evolution is consistently upward. This structural growth is captured by a log-linear trend model, which assumes a constant average percentage growth rate and reduces the influence of isolated project-driven peaks. This log-linear trend model is illustrated for neodymium (Nd) in **Figure 9**. The steeper increase observed in the direct-drive (DD) trend lines towards the end of the assessment period reflects the later and more rapid diffusion of DD technology in the Belgian wind turbine fleet compared to geared-box (GB) systems. Direct-drive turbines were deployed predominantly in more recent years, particularly in offshore projects, and are therefore associated with a more concentrated cohort of components and installations reaching end-of-life over a shorter time span. When evaluated using a log-linear trend model, this compressed deployment window translates into a higher estimated growth rate for DD-related end-of-life material flows, even if absolute volumes remain comparable to or lower than those of GB systems.

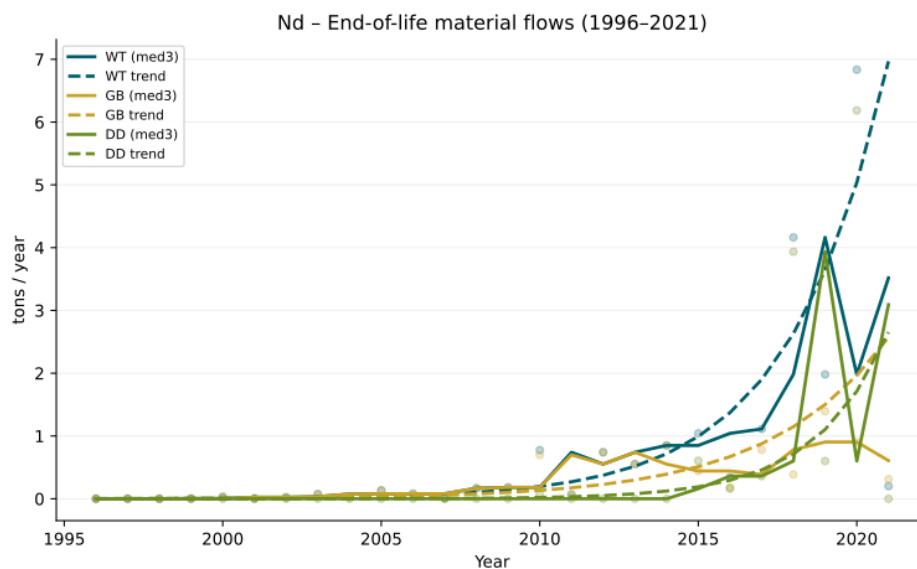


Figure 9: Illustration of the log-linear trend model applied to end-of-life (E1.6) neodymium (Nd) flows at the grandparent level (wind turbines, WT; blue) and parent level (gearbox-based, GB; yellow, and direct-drive, DD; green). Dotted lines indicate the estimated log-linear trends, while solid lines represent the three-year rolling median used to smooth the raw annual data prior to trend estimation.

Across the full 1997–2021 period, the use and stock of all metals exhibit strong growth. A comparison of growth rates between in-use material stocks (E1.1; **Figure 10**) and end-of-life flows (E1.6; **Figure 9**) highlights the dynamic nature of the Belgian wind turbine system. While in-use stocks of bulk metals increase at average annual rates of approximately 21–27%, and neodymium stocks at around 30%, the corresponding end-of-life material flows grow more moderately, at 13–17% per year. This divergence reflects the expansion phase of the system, in which material stocks accumulate rapidly as new capacity is installed, while end-of-life flows respond with a delay governed by turbine lifetimes and replacement cycles. The observed growth in E1.6 flows is therefore structurally linked to earlier stock accumulation and is expected to persist even under fluctuating future installation rates. These values align well with the trajectories observed at EU level, where increases in material flows entering the end-of-life phase have been attributed to a rapidly expanding in-use stock of wind turbines (León et al., 2025; Carrara et al., 2020).

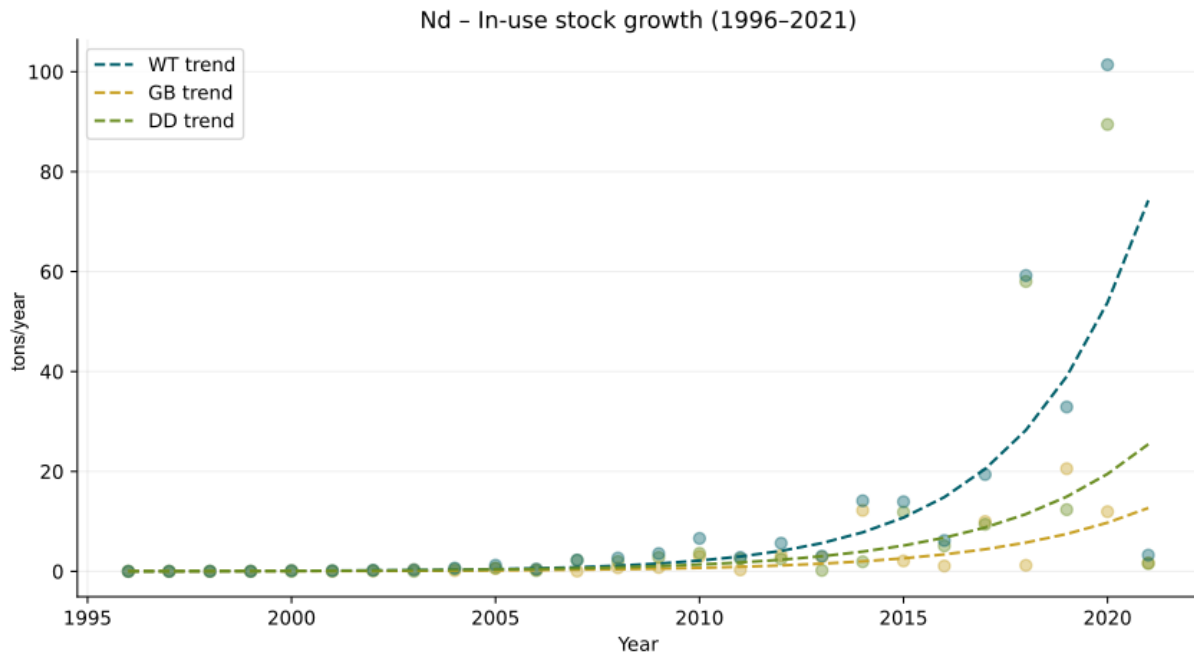


Figure 10: Log-linear trend model applied to the in-use stock of neodymium (Nd, E1.1) in the Belgian wind turbine fleet between 1996 and 2021. Dashed lines indicate log-linear trend estimates for the total wind turbine stock (WT) and for gearbox-based (GB) and direct-drive (DD) systems separately, based on annual stock data (points).

From a technological perspective, GB (gearbox) turbines historically dominate Belgian installations, especially onshore, which is reflected in higher E1.6B flows for Fe, Mn, Ni, and Al in earlier years. However, as offshore capacity expanded, the share of DD-PMSG turbines increased, leading to a marked rise in Cu and Nd flows associated with DD configurations. This is particularly visible after 2015, coinciding with large offshore wind projects in Belgian waters (FOD economie, 2025).

4 POLICY SUMMARY

The multilayer Material System Analysis (MMSA) applied in this study is highly relevant for Belgian policy makers because it connects technology deployment, material demand, and end-of-life management within one coherent analytical framework. Belgium is strongly dependent on imports for critical and strategic raw materials, while at the same time playing a key role in the European wind-energy value chain through wind deployment and specialised component manufacturing. The MMSA makes it possible to quantify how Belgian policy choices on technology deployment (e.g. drivetrain type, offshore versus onshore wind) directly translate into future material stocks, import dependencies, and waste streams.

Unlike conventional material flow analyses that focus on single materials in isolation, the multilayer approach captures interdependencies between multiple materials and technologies. This is particularly important for critical raw materials such as neodymium, copper and nickel, which are embedded in specific of complex and rapidly evolving technologies. By distinguishing between technology options, the methodology reveals how technology choices affect Belgium's exposure to supply risks and recycling challenges for different materials. As such, the MMSA provides policy-relevant evidence to support decisions on industrial strategy, circular economy policy, waste legislation, and raw-material security at both Belgian and EU levels.

Further refinement and broader application of the MMSA are important because Belgium's transition to climate neutrality will increasingly rely on multiple CRM-intensive technologies, not only wind turbines. Photovoltaics, batteries, electric vehicles and grid infrastructure all involve distinct material compositions, lifetimes and recycling pathways. Applying the methodology to additional case studies would allow policy makers to compare material bottlenecks and circularity potentials across technologies and to prioritise interventions where they are most effective.

Refining the methodology would also improve its policy usefulness. Key areas for refinement include better data on component trade (rather than only complete products), more detailed differentiation of steel grades and alloy compositions, and improved modelling of end-of-life treatment routes for critical materials. Such refinements would reduce uncertainty and enable more robust scenario analysis, for example to assess how changes in recycling technologies or design standards could improve material recovery and reduce import dependence over time.

Applying the MMSA to additional case studies would support forward-looking policy design. By linking historical deployment patterns to future end-of-life flows, the methodology allows anticipation of upcoming waste and recycling challenges before they materialise at scale. This anticipatory capacity is crucial for timely investments in recycling infrastructure, skills and innovation, and for avoiding future lock-ins that undermine circular-economy objectives.

The Belgian wind-turbine case study provides several insights that are directly relevant for policy. First, it demonstrates that material stocks embedded in the wind turbine fleet are expanding rapidly, with model-based average annual growth rates of approximately 21–30% for in-use stocks and 13–17% for end-of-life material flows across the analysed metals. This reflects the ongoing expansion phase of the system, in which material stocks accumulate faster than they are released at end-of-life. As a result, end-of-life material flows are expected to continue increasing structurally over the coming decades, even if annual installation levels fluctuate due to the project-based nature of wind turbine deployment.

Second, the results demonstrate that technology choice matters for material criticality. Gearbox turbines dominate historical installations and account for large shares of iron, manganese and nickel flows, whereas direct-drive turbines are strongly associated with copper and neodymium demand. In particular, neodymium flows are overwhelmingly linked to direct-drive permanent-magnet systems, creating a growing future waste stream of a material that is currently not functionally recycled in Europe.

Third, the study highlights a clear disconnect between growing end-of-life flows and circular recovery, especially for critical raw materials. While recycling rates for steel, iron, copper and aluminium are high, neodymium is entirely lost through downcycling into steel or slag. This means that, despite increasing availability of end-of-life material in Belgium, current waste management practices do not contribute to improving supply security for this critical metal.

Finally, the multilayer analysis reveals that Belgium's wind-energy system already constitutes a significant anthropogenic stock of strategic materials, particularly copper and neodymium. With appropriate policy support for design for recycling, targeted collection, and advanced recovery technologies, these stocks could become an important secondary resource in the future. Without such interventions, however, the growing material stocks risk turning into a long-term loss of critical raw materials, reinforcing import dependence rather than reducing it.

5 REFERENCES

Andersen, P.D., Bonou, A., Beauson, J., Brøndsted, P., 2014. *Recycling of wind turbines*. In: DTU International Energy Report 2014: Wind energy—Drivers and Barriers for Higher Shares of Wind in the Global Power Generation Mix. Technical University of Denmark.

Arcelormittal, 2024. *S355 structural steel grades for construction*. <https://constructalia.arcelormittal.com/en/steel-grades/s355>.

Bbf Associates, Kundig, K.J.A., 2011. *Market Study: Current and Projected Wind and Solar Renewable Electric Generating Capacity and Resulting Copper Demand*. Copper Development Association Inc

BIO by Deloitte, 2015, *Study on data for a raw material system analysis: roadmap and test of the fully operational MSA for raw materials.*, Prepared for the European Commission, DG GROW.

Carrara, S., et al., 2023, 'Supply chain analysis and material demand forecast in strategic technologies and sectors in the EU – A foresight study', JRC Publications Repository (<https://publications.jrc.ec.europa.eu/repository/handle/JRC132889>) accessed 21 May 2025.

Cullen, J.M., Allwood, J.M., Bambach, M.D., 2012. *Mapping the global flow of steel: from steelmaking to end-use goods*. *Environmental Science & Technology* 46 (24), 13048–13055. <https://doi.org/10.1021/es302433p>.

Darcy, J.W., Dhammika Bandara, H.M., Mishra, B., Blanplain, B., Apelian, D., Emmert, M.H., 2013. *Challenges in recycling end-of-life rare Earth magnets*. *JOM* 65 (11), 1381–1382. <https://doi.org/10.1007/s11837-013-0783-0>.

Demuytere, C., et al., 2024, 'Prospective material flow analysis of the end-of-life decommissioning: Case study of a North Sea offshore wind farm', *Resources, Conservation and Recycling* 200, p. 107283 (DOI: 10.1016/j.resconrec.2023.107283).

EngineerExcel, 2023. All About 18/8 Stainless Steel. EngineerExcel. <https://engineerexcel.com/18-8-stainless-steel/>.

Elsawy, E.E.T., EL-Hebeary, M.R., El Mahallawi, I.S.E., 2017. *Effect of manganese, silicon and chromium additions on microstructure and wear characteristics of grey cast iron for sugar industries applications*. *Wear (Lausanne)* 390–391, 113–124. <https://doi.org/10.1016/j.wear.2017.07.007>.

European Commission: Joint Research Centre, 2020a, *Raw materials demand for wind and solar PV technologies in the transition towards a decarbonised energy system*, Publications Office (<https://data.europa.eu/doi/10.2760/160859>).

European Commission: Joint Research Centre, 2020b, *Revision of the material system analyses specifications*, Publications Office (<https://data.europa.eu/doi/10.2760/374178>).

Farina, A. and Anctil, A., 2022, 'Material consumption and environmental impact of wind turbines in the USA and globally', *Resources, Conservation and Recycling* 176, p. 105938 (DOI: 10.1016/j.resconrec.2021.105938).

FOD economie, *Belgische windenergie op zee*, accessed 12/9/2025, (<https://economie.fgov.be/nl/themas/energie/bronnen-en-dragers-van-energie/belgische-windenergie-op-zee>).

Godoy León, M. F., et al., 2025, 'Multilayer Material System Analysis of wind turbines: correlation of stocks and flows in the EU of six metals and two drivetrain technologies', *Journal of Cleaner Production* 518, p. 145794 (DOI: 10.1016/j.jclepro.2025.145794).

Grohol M. and Veeh C., 2023, *Study on the Critical Raw Materials for the EU 2023 - Final report*, No 978-92-68-00414-2, European Commission (10.2873/725585).

Kawecki, D., Scheeder, P.R.W., Nowack, B., 2018. *Probabilistic material flow analysis of seven commodity plastics in Europe*. *Environmental Science & Technology* 52 (17), 9874–9888. <https://doi.org/10.1021/acs.est.8b01513>.

Matos, C.T., et al., 2020, 'Material system analysis: a novel multilayer system approach to correlate EU flows and stocks of Li-ion batteries and their raw materials.', 26 (4), pp. 1261-1276.

Müller, E., et al., 2014, 'Modeling Metal Stocks and Flows: A Review of Dynamic Material Flow Analysis Methods', *Environmental Science & Technology* 48(4), pp. 2102-2113 (DOI: 10.1021/es403506a).

Nelen D., Margot C., Deckers J. (2025) Case study on critical raw material flows for Belgium. Mapping critical raw material flows in Belgium: focus on Platinum Group Metals (PGM) and nickel. Final Report. Brussels: Belgian Science Policy Office 2023 (BRAIN-be 2.0 - (Belgian Research Action through Interdisciplinary Networks))

Pauliuk, S., et al., 2017, 'Regional distribution and losses of end-of-life steel throughout multiple product life cycles—Insights from the global multiregional MaTrace model', *Resources, Conservation and Recycling* 116, pp. 84-93 (DOI: 10.1016/j.resconrec.2016.09.029).

Reliance foundry, 2020. *Introduction to Cast Iron: History, Properties, and Uses*. Reliance Foundry Co. Ltd. <https://www.reliance-foundry.com/blog/cast-iron>.

RystadEnergy, 2023. *State of the European wind energy supply chain. A «what-would-it- take» Analysis of the European Supply Chain’s Ability to Support Ambitious Capacity Targets Towards 2030.*

Savvidou, G., Johnsson, F., 2023. Material

Shammugam, S., et al., 2019, ‘Raw metal needs and supply risks for the development of wind energy in Germany until 2050’, *Journal of Cleaner Production* 221, pp. 738-752 (DOI: 10.1016/j.jclepro.2019.02.223).

thyssenkrupp. *Unalloyed and alloyed quenched and tempered steels – high strength and ductility after hardening for highly stressed components.* <https://www.thyssenkrupp-steel.com/en/products/hot-strip/c-steel/unalloyed-and-alloyed-quenched-and-tempered-steel/unlegierter-und-legierter-verguetungsstahl.html>.

Yang, Y., Walton, A., Sheridan, R., Güth, K., Gauß, R., Gutfleisch, O., Buchert, M., Steenari, B.-M., Van Gerven, T., Jones, P.T., Binnemans, K., 2017. *REE recovery from end-of-life NdFeB permanent magnet scrap: a critical review.* *J. Sustain. Metall.* 3 (1), 122–149. <https://doi.org/10.1007/s40831-016-0090-4>.

6 ANNEXES

Table 8 : Mass proportions (%) per component (upper table) or subassembly (lower table) adopted from Shammugam et al. (2019).

	Pitch	Yaw	Gearbox	Generator				
				GB-DFIG	DD-PMSG	GB-PMSG	DD-EESG	GB-SCIG
low alloyed steel	27.1%	25.9%	10.2%	68.2%	64.1%	40.4%	44.3%	68.2%
high alloyed steel	16.8%	41.6%	39.2%	0.6%	0.5%	0.3%	0.4%	0.6%
cast iron	51.5%	23.5%	48.6%	3.7%	3.5%	2.2%	2.4%	3.7%
copper	0.1%	0.0%	0.0%	6.7%	4.0%	7.6%	11.7%	6.7%
aluminium	1.4%	5.1%	2.00%	0.4%	0.4%	0.2%	0.3%	0.4%
EE		3.0%		2.0%	1.9%	1.2%	1.3%	2.0%
iron				17%	24%	46%	38.5%	16.7%
magnets (kg/MW)				-	650	120	-	
others	3.1%	0.9%	0.0%	1.7%	1.7%	2.6%	1.1%	1.7%
Total	100.0%	100.0%	100.0%	100.0%	100.0%	100.0%	100.0%	100.0%

	Rotor	Nacelle					Tower
		GB-DFIG	DD-PMSG	GB-PMSG	DD-EESG	GB-SCIG	
low alloyed steel	9.8%	20.7%	8.9%	10.3%	8.9%	12.5%	97.1%
high alloyed steel	9.4%	36.1%	29.8%	39.3%	29.8%	41.1%	-
cast iron	25.8%	35.6%	52.6%	41.5%	52.6%	35.6%	-
copper	0.1%	2.1%	2.2%	2.2%	7.7%	3.2%	0.9%
aluminium	0.1%	1.1%	0.9%	0.9%	0.9%	1.0%	1.0%
EE		0.3%	0.1%	0.4%	0.1%	0.6%	1.0%
others	54.8%	4.1%	5.5%	5.4%	0.0%	6.0%	0.0%
Total	100.0%	100.0%	100.0%	100.0%	100.0%	100.0%	100.0%